# Multiphoton-Excited Fluorescence

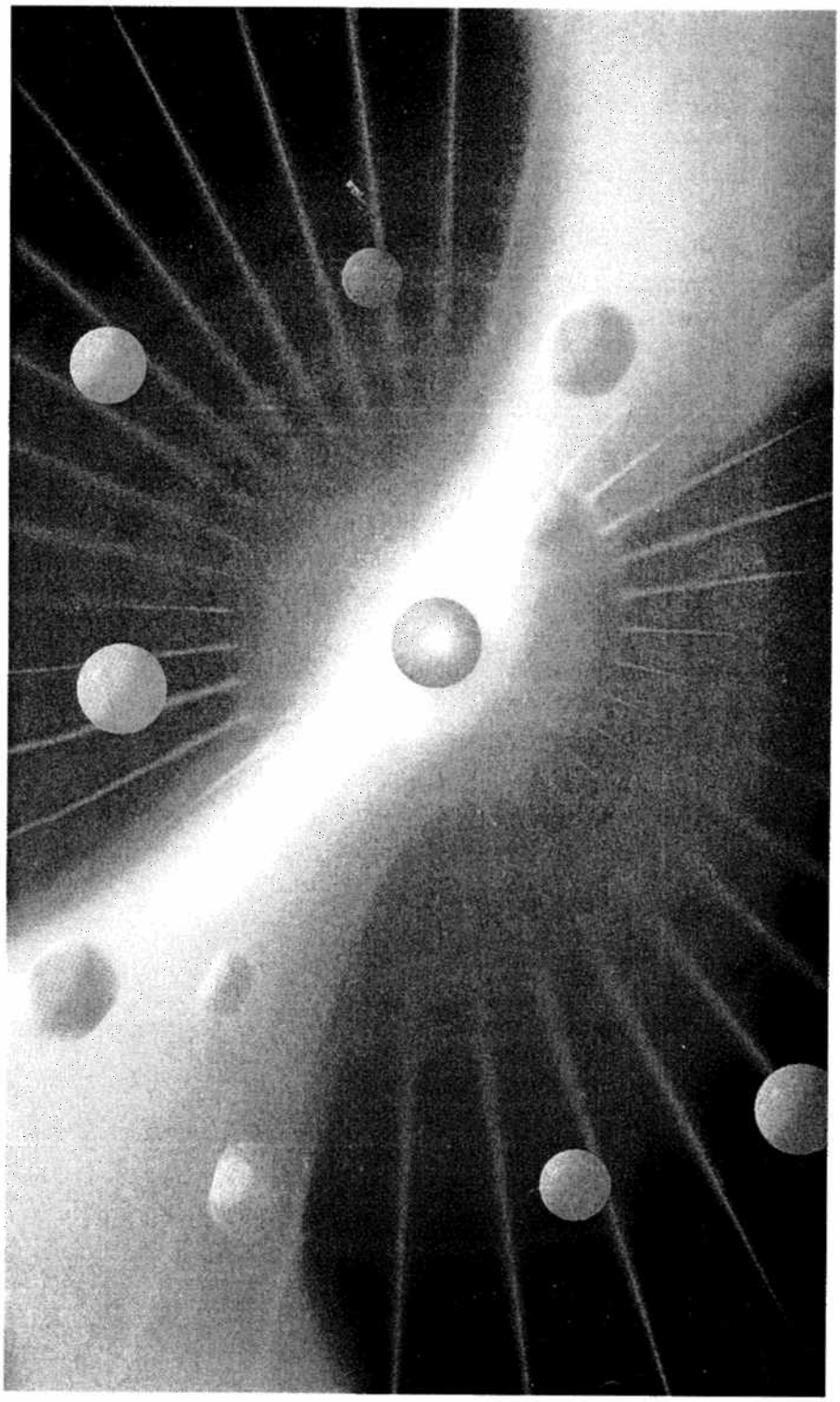

The recent development of "turnkey" femtosecond pulsed-laser sources has broadened the analytical applications of fluorescence analysis, making it straightforward to excite emission from molecules through the essentially simultaneous absorption of multiple, relatively low-energy photons. This new spectroscopic tool, multiphoton-excited (MPE) fluorescence (Figure 1), offers several benefits over standard single-photon excited (1PE) fluorescence for high-sensitivity spectroscopic and microscopic analyses. Opportunities now exist for probing chemistry and structure deep within biological tissue, for performing sensitive measurements on deep-UV ($\lambda_{ex} \approx$ 200–300 nm) chromophores and spectroscopically diverse components within a mixture or specimen, and for initiating chemical reactions in femtoliter volumes. This Report briefly considers some of the unique properties and practical aspects of this alternative spectroscopic approach and discusses recent bioanalytical applications in microscopy and microcolumn separations that have benefited from MPE fluorescence. More technical and complete treatments on multiphoton excitation can be found both as primary literature and in review format (*1–9*).

## ABCs of multiphoton excitation

In a certain sense, the electronic excitation of a chromophore through absorption of a photon or photons can be considered a reversible chemical "reaction" in which the reactant and product share the same atomic components and connectivity but differ in electronic geometry. This can be represented in standard chemical equation format as

$$M + n(h\nu) \rightleftarrows M^* \qquad (1)$$

where M and $M^*$ are the ground- and excited-state chromophores, respectively.

**Jason B. Shear**
*University of Texas, Austin*

# in Bioanalytical Chemistry

$h\nu$ is a photon, and $n$ is the number of photons that must be absorbed for excitation to take place. Both forward and back reactions are "catalyzed" by the electric field; hence, the back reaction in equation 1 represents stimulated emission as opposed to fluorescence. As with a simple chemical reaction requiring a multiparticle collision, the rate of product formation can be stated in terms of the reactant concentrations:

$$d[M^*]/dt = k[h\nu]^n[M] = \delta I^n[M] \quad (2)$$

where $k$ is the forward rate constant and $I$ is the instantaneous intensity of the excitation light (in units of photons $s^{-1}$ $cm^{-2}$). The excitation cross section, $\delta$, is proportional to $k$ and has units that depend on the number of excitation photons ($cm^{2n}$ (s/photon)$^{n-1}$). Because the excitation rate, $d[M^*]/dt$, is proportional to measured fluorescence $F$, the photon dependence of an excitation process can be determined empirically from the slope of a log$F$ versus log$I$ plot (provided no significant depletion of [M] is produced).

From equation 2, it is evident that multiphoton excitation depends more strongly on excitation intensity than does single-photon excitation. If we consider the excitation process in Figure 1, absorption of two photons is depicted as a sequential process that passes through a "virtual state"—a superposition of energy levels that exists for extremely short times as a consequence of Heisenberg broadening of states. (As with position and momentum, energy and time are conjugate variables in the uncertainty inequality.) For two-photon absorption to take place, a molecule elevated to a virtual state must interact with a second photon within ~1 fs. Otherwise, the virtual state dissipates, and the molecule relaxes back to the ground electronic manifold. Depending on the vibrational level into which the molecule returns, this relaxation results in elastic or inelastic light scattering.

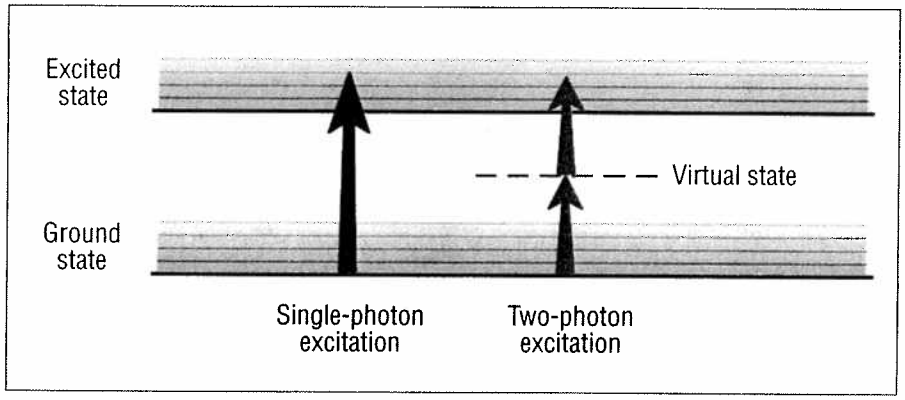


**Figure 1. Excitation of molecular chromophores using single-photon excitation and multiphoton excitation.**

In single-photon excitation, the energy of the source photons must equal the energy gap between electronic levels. In this simplified representation, the same energy gap can be bridged through the nearly simultaneous absorption of two photons that each have half the energy (i.e., twice the wavelength) as the photon used for single-photon excitation. The multiphoton transition often is depicted as passing through one or more "virtual" states that persist for extremely brief periods according to uncertainty broadening of molecular energy levels.

The significance of the $I^n$ dependence can be appreciated by considering a focused laser beam with a position of highest intensity at the focal point (Figure 2). Because each plane perpendicular to the propagation axis experiences the same total photon flux (photons $s^{-1}$), single-photon excitation generates the same total excitation (and hence, fluorescence) in every plane through which the light propagates. However, when a nonlinear relationship exists between the excitation rate and the light intensity, all planes are no longer equal—those closest to the focal point support more excitation events. The axial- and radial-multiphoton excitation gradients depend on how tightly the light is focused and whether Gaussian or diffraction-limited optics are used. For high numerical aperture (NA) diffraction-limited focusing, probe volumes can be produced that are <1 $\mu m^3$.

Some early analytical applications used continuous-output lasers to achieve multiphoton excitation (*10*); however, because high (average) power usually is needed to achieve reasonable multiphoton excitation with such sources, they are rarely used today (*11*). For two-photon chromophores with large cross sections, such as fluorescein and rhodamine B, hundreds of milliwatts of continuous-output light must be tightly focused to achieve high excitation rates. Even in these favorable instances, the required power is often great enough to damage cellular specimens through heating and single-photon-induced photoreaction of cellular components (e.g., cytochromes). High powers also make rejection of the long-wavelength scatter more challenging, and detection sensitivity may be degraded. The power required for continuous-output excitation is often too large to analyze two-photon fluorophores with small excitation cross sections.

The average power required for multiphoton excitation can be dramatically reduced by using a pulsed-laser source in place of a continuous source (*8*). The critical parameter for achieving multiphoton excitation is instantaneous intensity, not the time-averaged intensity (no distinction is made for single-photon excitation). Hence, for a given time-averaged source output (i.e., as would be measured by a

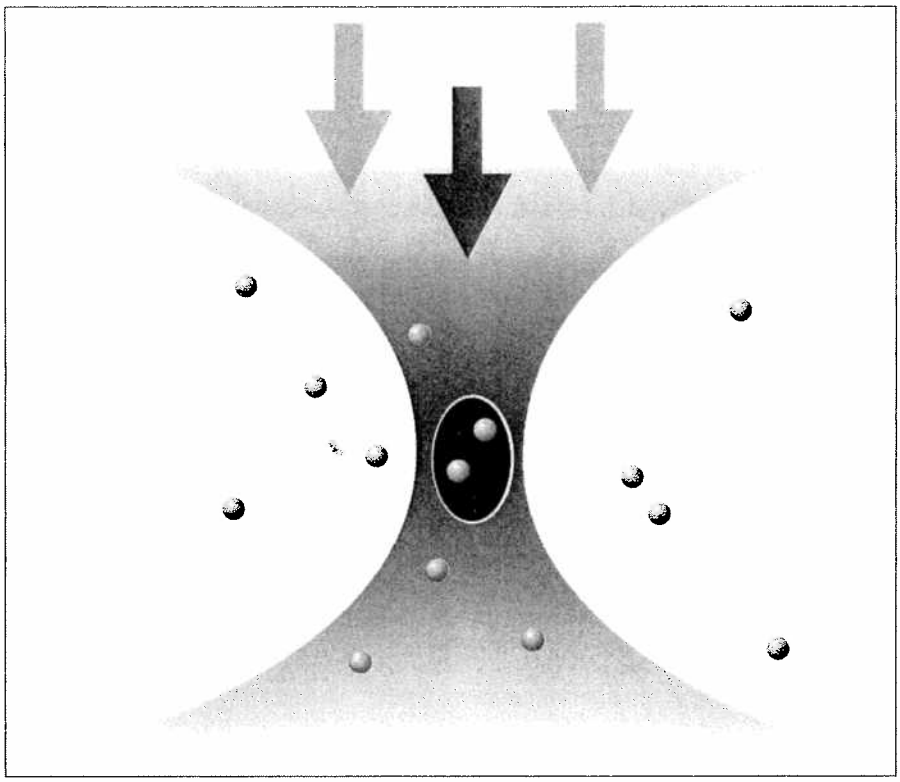

**Figure 2. Spatial localization of multiphoton excitation using tightly focused laser light.**

The high-intensity dependence of multiphoton excitation can confine fluorescence and photochemical reactions to spatial coordinates in proximity to the focal point (region depicted as a black oval) when focusing light with high-NA optics.

power meter with a slow rise time), more excitation events are obtained when the source photons are "focused" into discrete temporal packets than when they are delivered in a continuous stream. Indeed, the smaller the laser duty cycle (defined as the fraction of time the laser is in the "on" state), the greater the total number of molecular excitations. Quantitatively, when using an idealized square-pulse laser under nonsaturating conditions, it can be shown that

$$N_{\text{pulsed}}/N_{\text{CW}} = D^{1-n} \qquad (3)$$

where $N_{\text{pulsed}}$ and $N_{\text{CW}}$ are the number of molecules excited in a given period (at least many pulse cycles long) using pulsed and continuous-output sources, respectively, and $D$ is the duty cycle of the source (by definition, $0 \leq D \leq 1$). For single-photon excitation, this relationship gives the expected result that pulsed and continuous-output sources yield equivalent fluorescence signals. For nonlinear excitation, the enhancement derived from pulsed excitation increases sharply with the number of photons required for excitation.

Although it is instructive to consider the nonsaturating regime in which only a small fraction of molecules is excited at any time, for many practical applications a more thorough sampling of the molecular population can be advantageous, particularly when sensitivity is an issue. When high sensitivity is required, one typically obtains the best detection limits when a substantial fraction of analyte molecules is excited by each laser pulse (provided that background sources do not scale more strongly with excitation intensity than does fluorescence) and when excitation pulses are separated in time by approximately the excited-state lifetime (typically 0.1–10 ns in aqueous solution). In this way, molecules are rapidly cycled through an excited state many times before they can diffuse (or migrate in an externally applied field) to positions outside the probe volume.

To illustrate the effect of pulse repetition rate, consider excitation of a fluorophore with an excited-state lifetime of 10 ns using a laser that produces 1-ns square pulses 10 times/s, each containing 1 mJ of energy. Here, the duty cycle is low ($D \approx 10^{-8}$), and the instantaneous power is large during a pulse ($P_{\text{inst}} \approx 10^{6}$ W) even though the time-averaged output from the laser is relatively low ($P_{\text{avg}} \approx 10^{-2}$ W). Nevertheless, a fluorophore can be excited only once each pulse at best (i.e., once every 100 ms). If the mean diffusion time through a (focused) probe volume is less than this delay period between pulses, a given molecule is unlikely to be excited even a single time, and detection sensitivity will be extremely poor. In contrast, a high repetition rate laser that pulses 100 million times/s potentially could excite the molecule ~$10^{7}$ times within a 100-ms diffusion period. Note that the combined characteristics of high repetition rate and low duty cycle are obtained only in lasers with extremely short pulse durations (picoseconds to femtoseconds).

Before the 1990s, reliable, high repetition rate, low duty cycle lasers in the needed wavelength regions were not commercially available. A few sources with appropriate characteristics did exist, such as the colliding pulse mode-locked dye laser, but these lasers were often challenging to operate even for technically skilled personnel. This situation improved dramatically with the introduction of the mode-locked, wavelength-tunable titanium:sapphire (Ti:S) laser (*12*).

The solid-state Ti:S oscillator typically is pumped by a standard $Ar^{+}$ laser or by a frequency-doubled neodymium:vanadate laser, yielding a highly reliable laser system with low relative root mean square noise (~1%). In the standard configuration, pulses of ~100-fs duration (and 10-nm bandwidth) pass through the laser's output coupler each time the light makes a round-trip pass through the laser cavity (~10–15 ns), yielding a low duty cycle (~$10^{-5}$) with extremely high instantaneous powers at low average power outputs. With cavity optics designed for broad tunability, and some means to alter the relative gain in the cavity for desired wavelengths, the output wavelength of Ti:S lasers can be tuned continuously over a broad spectral range. When using high-NA optics, a 10-mW Ti:S laser beam can be focused to produce an instantaneous intensity of ~$10^{11}$ W cm$^{-2}$ at the focal point.

Xu and Webb have performed extensive measurements of the two-photon fluorescence excitation spectra for many common fluorescent dyes in aqueous and alcohol solutions, and other researchers have measured two- and three-photon excitation spectra for biological fluorophores (*13–17*). Fortuitously, most fluorophores ordinarily excited by single photons of visible light have two-photon excitation maxima within the tuning range of the Ti:S laser (~700–1000 nm). In the simplest approximation, one might expect to find two-photon excitation maxima at twice the wavelength of the single-photon excitation peaks; however, because the selection rules for excitation depend on various molecular properties and the number of photons involved in the absorption event, the shape of multiphoton excitation spectra in general cannot be predicted simply from measured single-photon excitation spectra. In contrast, emission spectra generated using single-photon excitation and multiphoton excitation are almost always identical to within experimental error because fluorescence typically takes place after relaxation to the ground vibrational level of the lowest excited electronic manifold.

Experimentally, it has been found that for most fluorophores

$$\delta_f \leq 10^{-15}\text{cm}^{2n}(10^{-33}\text{s/photon})^{(n-1)} \quad (4)$$

where $\delta_f$ is the fluorescence action cross section (equivalent to excitation cross section × fluorescence quantum yield). Thus, cross sections for high-efficiency laser dyes are approximately $10^{-15}$ cm$^2$ (1PE fluorescence), $10^{-48}$ cm$^4$ s photon$^{-1}$ (2PE fluorescence), and $10^{-81}$ cm$^6$ s$^2$ photon$^{-2}$ (3PE fluorescence). As a shorthand for discussing two-photon cross sections, the unit of $10^{-50}$ cm$^4$ s photon$^{-1}$ has been defined as 1 Göppert-Mayer (GM; named for Maria Göppert-Mayer, who predicted nonresonant multiphoton excitation in 1931).

A wide range of synthetic molecules have peak two-photon cross sections large enough to serve as sensitive indicators for biological molecules at powers compatible with live cellular imaging, and a handful of the best dyes, including DiI, Calcium-Green, Calcium-Crimson, and some BODIPY- and coumarin-based probes, have cross sections in excess of 10 GM. In addition, experimentalists and theoreticians recently have collaborated on engineering dyes with enhanced two-photon cross sections (*18*). Action cross sections for native biological fluorophores are generally much lower than for engineered dyes; NADH, for example, has a maximum two-photon cross section of ~0.01 GM (*17*), and tryptophan has a peak three-photon cross section of ~$10^{-84}$ cm$^6$ s$^2$ photon$^{-2}$ (*15*). Because multiphoton cross sections are small, the excitation power needed to reach chromophore saturation (i.e., one excitation per molecule per laser pulse) in general increases substantially with the number of photons that must be absorbed to promote a transition (*17*). For two-photon excitation, usually <50 mW of near-IR Ti:S laser light must be focused to perform high-sensitivity measurements—levels that do not cause significant temperature increases of most aqueous samples (*19*).

## Deep-tissue imaging

In 1990, Denk, Strickler, and Webb adapted a laser-scanning confocal microscope to deliver subpicosecond pulses of laser light to a specimen in place of standard Ar$^+$ laser radiation (*20*). As discussed, the dependence of excitation on multiple photons provides a strong 3-D localization of the probe region when focusing the laser beam with high-NA optics. Similar to confocal spatial filtering, this localization allows one to section a microscopic specimen optically by raster-scanning the focal point within a plane perpendicular to the laser propagation axis, collecting fluorescence and background photons from a tightly confined spatial region at each step position. After this "*x–y*" scan is performed, the specimen can be shifted minute distances along the *z* axis (laser-propagation axis) to acquire additional optical sections—each as thin as ~1 µm—at different planes within the specimen. Once an entire 3-D array of points is accumulated, reconstruction algorithms can be used to generate views of the specimen from any desired perspective. Distinct from the confocal approach, multiphoton excitation achieves 3-D resolution by strongly confining the region in which excitation takes place. This can be important in limiting the spatial extent of photobleaching and photodamage in specimens. Moreover, the unique characteristics of multiphoton excitation can open new windows for probing structure and chemistry deep within living specimens.

High-resolution imaging deep within biological tissue has presented severe challenges for microscopists. It is often difficult to deliver UV and visible excitation light to coordinates deep within tissue because of absorption and scattering, and it is even more problematic to adequately collect the fluorescence that is generated. Confocal imaging achieves 3-D sectioning by focusing the fluorescence generated at or near the laser focal point at a small pinhole placed in front of a detector, thus rejecting fluorescence/scatter that originates elsewhere in the specimen (*21*). However, even fluorescence produced at the focal point is likely

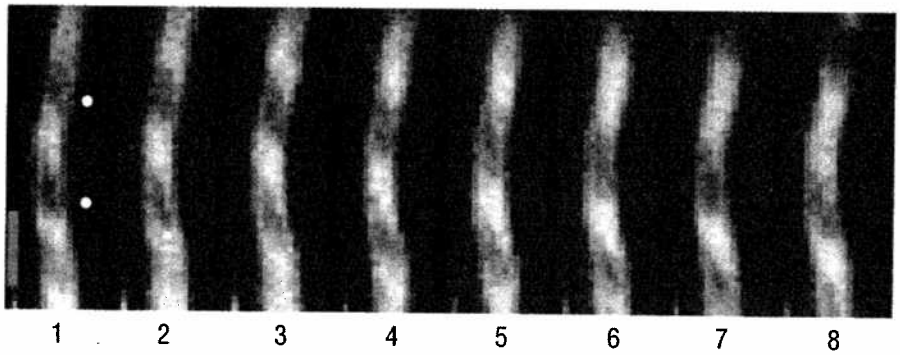


**Figure 3. Multiphoton fluorescence imaging of structures deep within living biological tissue.**

The movement of nonfluorescent red blood cells (RBCs) can be seen in these successive images (shown left to right) acquired every 16 ms at a depth of 450 µm into the pia of a rat neocortex. Two RBCs can be identified readily as dark objects (next to white circles outside the capillary in Frame 1) in a background of fluorescein-labeled serum and move downward in Frames 2–8. Green scale bar (lower left) is 10 µm. (Adapted with permission from Ref. 22.)

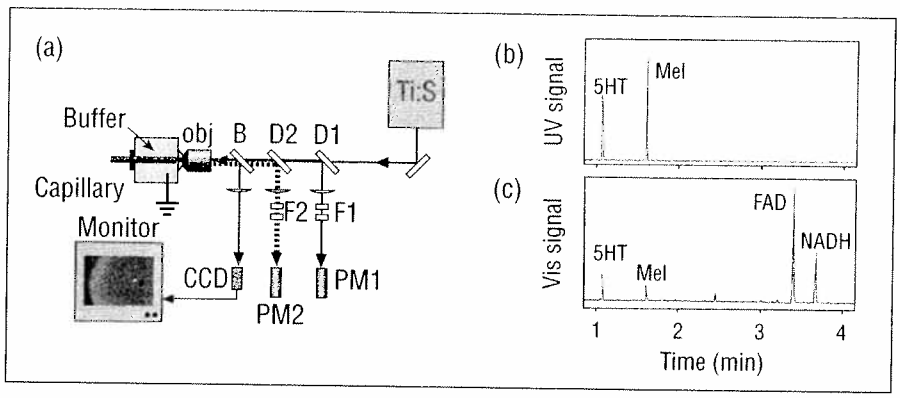


**Figure 4. Analysis of mixtures containing spectrally diverse biological fluorophores using CE with MPE fluorescence detection.**

(a) Block diagram of the MPE fluorescence apparatus. Output from the Ti:S laser (typically 50- to 100-mW average power) is directed through a series of beamsplitters and dichroic mirrors into a high-NA microscope objective (obj), which focuses the light into the grounded outlet reservoir (containing electrophoresis buffer). Fluorescence from analytes migrating out of the capillary is collected using the same objective and is reflected to photomultiplier tubes (PM1, PM2) by dichroic mirrors D2 (UV fluorescence) and D1 (visible fluorescence). UV band-pass filters (F2) and visible-passing filters (F1) are used to isolate fluorescence from laser scatter. The end of the capillary is imaged onto a charge-coupled device (CCD) video camera, providing a means to overlap the channel aperture with the laser focal point. In the image on the monitor, the focal point is slightly misaligned and is seen as a reflection from the capillary surface. After the capillary is positioned by a multiaxis micropositioner, the beamsplitter (B) is removed. (b) Three-photon excitation of serotonin (5HT) and melatonin (Mel) produces fluorescence that can be measured in a UV detection channel after separation in an electrophoresis field of several hundred volts per centimeter (5-μm i.d. capillary). (c) The electropherogram produced by the visible detection channel (same electrophoresis separation) shows 2PE fluorescence of NADH and FAD, and peaks caused by the rapid photochemical conversion of 5HT and Mel to visible-emitting products. (Adapted from Ref. 23.)

to be rejected by this spatial filter if the emission is scattered before exiting the tissue. Such problems are greatly ameliorated in multiphoton microscopes. The near-IR excitation light is absorbed poorly by most biological chromophores (except near the focal point) and is scattered much less efficiently than UV and visible light. Moreover, MPE fluorescence is collected in a wide-field geometry—an approach that is far less sensitive to scattering of emitted light.

Researchers at the University of California–San Diego and Bell Laboratories recently published a striking demonstration of deep-imaging capabilities using 2PE fluorescence (*22*). Images within the cerebral cortex of live rats were acquired by focusing 830-nm light through openings created in the crania. High-resolution images could be collected at depths ~0.6 mm below the surface pia—several hundred micrometers deeper than previously imaged using confocal microscopy. Sequences of images taken at twice the video rate revealed the movement of nonfluorescent objects through capillaries within the brain (Figure 3), an observation interpreted as the flow of red blood cells. Tactile stimulation of the animals' hind limbs and facial vibrissae (whiskers) could be correlated with transient increases in the flux of red blood cells through capillaries in distinct regions of the cortex.

## Multifluorophore sensing

To more fully gauge the chemical and physical state of living, dynamic cells, microscopists increasingly are performing analyses on multiple fluorophores that possess distinct spectroscopic signatures. These fluorescent molecules may be natively fluorescent biological species (e.g., NADH and tryptophan) or exogenous probes that report on some property when incorporated into cells (e.g., the calcium-sensitive dyes). To facilitate the sensitive analysis of several fluorophores simultaneously using standard single-photon excitation, selected dyes should have distinct emission wavelengths but similar peak-excitation wavelengths. Although multiple sources could be used to excite chromophores with disparate absorption maxima, this approach would complicate discrimination of fluorescence from laser scatter. Unfortunately, one does not often have the luxury to choose fluorescent probes on the basis of restrictive photophysical characteristics.

The difficulties associated with multifluorophore analysis can be surmounted with multiphoton excitation. Experiments performed in the laboratory of Watt Webb at Cornell University demonstrated that four spectrally distinct fluorescent dyes could be analyzed in cultured cells using a single-excitation wavelength from a Ti:S laser (*17*). Images of rat basophilic leukemia (RBL-2H3) cells revealed the plasma membrane (pyrene-labeled phospholipid), nuclear material (DAPI), the Golgi (BODIPY-labeled sphingomyelin), and mitochondria (rhodamine 123). Sensitive one-photon analysis of all these dyes would be challenging, because excitation maxima span more than 150 nm in the mid-UV (pyrene, DAPI) and visible (BODIPY, rhodamine 123) spectral regions. In contrast, all four species can be excited efficiently using two photons of 705-nm light. Although this excitation energy ($\sim 2 \times 1.65$ eV = 3.30 eV) is similar to optimal one-photon energies for pyrene and DAPI, it corresponds to very weak one-photon absorption bands for rhodamine 123 and BODIPY. Fortunately, differences in selection rules for single- and two-photon excitation of rhodamine 123 and BODIPY enhance the intensity of the higher-energy transitions relative to the standard low-energy bands.

Certainly, fortuitous changes in transition strengths cannot be expected in all instances, but many important dyes have significant two-photon excitation cross sections in the 700- to 750-nm range. Moreover, because two-photon excitation light typically is several hundred nanometers longer than emission, the excitation wavelength can be chosen irrespective of overlap between the excitation energy ($E_{ex} = 2 \times hc/\lambda_{ex}$) and the fluorescence energy spectra of the dyes. In one-photon multifluorophore experiments, one often must compromise when selecting the excitation source—overlap of the excitation energy/wavelength with significant emission from any fluorophore will increase the measured background and degrade detection limits.

Chromophores with even greater spectroscopic diversity can be analyzed by exciting transitions with different numbers of Ti:S photons. For example, the indoles serotonin (5HT) and melatonin have large ground- to excited-state energy gaps (~4–6 eV),

whereas the redox cofactors NADH and FAD have relatively small energy gaps (~2.7–3.5 eV). We demonstrated that these four compounds could be analyzed in a single capillary electrophoresis (CE) separation by exciting the indoles with three photons and the cofactors with two photons of 750-nm light from a Ti:S laser and by detecting fluorescence in separate UV and visible-emission channels (*23*). To overcome optical aberrations inherent to focusing light tightly through the curved surface of the capillary, an end-column epi-illumination geometry was developed to allow the use of high-NA focusing optics (Figure 4a). In addition to the expected fluorescence of 5HT and melatonin in the UV detection channel (Figure 4b), these compounds also yield emission that is detected in the visible channel along with fluorescence from the two-photon species, NADH and FAD (Figure 4c). Interestingly, the 5HT and melatonin peaks in Figure 4c are not caused by channel cross-talk, but rather by multiphoton-induced photoreaction and subsequent 2PE fluorescence of the reaction products. As discussed later, this five- to six-photon process can be enhanced and quantitatively controlled, providing a useful detection strategy for various indoles fractionated by CE.

## UV fluorescence

Sensitive measurements of deep-UV fluorophores ($\lambda_{ex} \approx$ 200–300 nm) traditionally have posed serious challenges for bioanalytical chemists. Extremely high UV-scattering cross sections and luminescence from optics and filters often degrade signal-to-noise ratios, and photodamage to living specimens by highly energetic photons can compromise cell viability. Moreover, production and control of light in this spectral region can be problematic. Recent studies suggest that these obstacles to efficient, sensitive detection of biological fluorophores can be circumvented to a large extent by using multiphoton excitation.

Scanning microscopy experiments performed at Cornell University demonstrated the value of MPE UV fluorescence in determining 5HT content, distribution, and secretion from cultured RBL-2H3 cells (*15, 24*). This cell system has been a particularly useful model for studying secretion in mammalian cells, with a well-characterized sequence of biochemical and morphological responses to chemical stimulation that culminate in exocytosis (*25*). In an initial test of feasibility, we performed "cuvette" studies to map out the 3PE fluorescence spectrum of 5HT in the approximate wavelength range 700–900 nm (energies corresponding to single-photon excitation with ~235–300 nm light). Although no significant three-photon excitation was observed for energies corresponding to the $S_0 \rightarrow S_1$ transition (expected at ~3 × 300 nm = 900 nm), the excitation efficiency increased dramatically as the laser was tuned toward its short-wavelength limit. With this spectral information in hand, initial 3PE images of RBL-2H3 cells were acquired using 710-nm excitation. These experiments showed that the 5HT content of RBL-2H3 cells typically is low, although we observed that some cells synthesize and package a UV-fluorescent species, presumably 5HT, into large cytosolic granules. Because most RBL-2H3 cells can accumulate exogenous 5HT into existing histamine granules by sequential transport across the plasma and granular membranes, this cell line provided an opportunity to study both uptake and stimulated release of 5HT.

By using a 1.3-NA microscope objective to focus the Ti:S beam within cultured cells, we acquired high-resolution 3-D images of relatively large secretory granules (or clusters of granules) loaded with exogeneous 5HT. We found that when RBL-2H3 cells were bathed in submicromolar 5HT for several hours, granular 5HT content would rise to ~50 mM. Total cellular 5HT content and the spatial distribution of granules were variable but could be determined readily in individual cells. From 3-D reconstructions, we observed that in some cells granules appeared to be distributed in a largely random fashion throughout the cytosol, and in other instances they were localized to specific regions (Figure 5a). Although 5HT granules could be best imaged by using 700- to 710-nm Ti:S light, we were unable to reproducibly evoke secretion from cells subjected to a 3-D multiphoton excitation laser scan using these wavelengths. For this application, the capability of multiphoton excitation to promote transitions of substantially different energies was an impediment to our

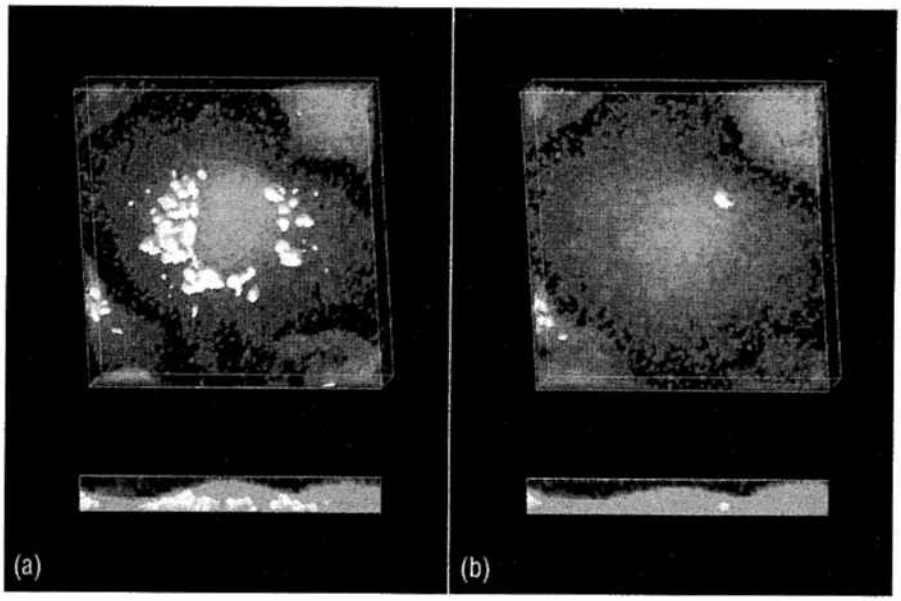


**Figure 5. Multiphoton excitation UV fluorescence of serotonin in a cultured RBL-2H3 cell.**

A focused Ti:S laser beam was raster-scanned in a sample plane perpendicular to the laser propagation axis; subsequent focal planes were examined by stepping the fine focus knob on the microscope using a motorized drive. (a) 3-D reconstructions of a cell initially containing numerous large serotonin secretory granules (white structures), with views from the top (large box) and side (small box). Note that the granules are clustered mostly near the base of the cell. To generate these images, the 3PE fluorescence of serotonin was measured in 15 sequential planes acquired at 1-μm steps through the cell. (b) Same 3-D reconstructions 10 min after degranulation was stimulated by cross-linking cell surface IgE receptors. (Adapted with permission from Ref. 24.)

goals. At the same time that 5HT fluorescence was excited through the absorption of three photons, molecules critical to cellular viability—including NAD(P)H and FAD—were undergoing two-photon-promoted photoreactions. Fortunately, by tuning the Ti:S laser to 740 nm, the photodamage pathways could be suppressed and degranulation evoked (Figure 5b). When 3-D data was not desired, sequential (planar) images could be acquired every few seconds to track the time course of large granule exocytosis. In many instances, the release rate of 5HT followed an oscillatory pattern with a period of ~90 s, a result in general agreement with extracellular amperometric measurements made using carbon-fiber microelectrodes (*26*).

In the past several years, Yeung and coworkers have demonstrated impressive capabilities for UV imaging of 5HT in cultured cells using single-photon excitation (*27, 28*). Thus far, the relative merits of single-photon excitation and multiphoton excitation for UV fluorescence imaging have yet to be conclusively determined. Although it is clear that multiphoton excitation can virtually eliminate several sources of background normally associated with UV excitation, limiting photobleaching and photodamage is less clear. For example, it is likely that the quantum yield of photobleaching/photodamage in many instances is smaller for UV excitation than for multiphoton excitation (perhaps as a result of higher-order absorption events). However, multiphoton excitation can limit undesirable photoprocesses to well-defined 3-D coordinates or selected planes within a specimen, a fact that may offer advantages in maintaining cellular viability.

UV-excited fluorescence has been less profitable as a high-sensitivity detection strategy for tyrosine derivatives than for indoles, mostly because of poor one-photon absorption cross sections for $S_0 \rightarrow S_1$ transitions, small Stokes shifts (~30 nm), and short emission wavelengths. Although low attomole quantities of 5HT and other indoles can be detected by using UV-excited fluorescence with microcolumn separations, mass detection limits for catecholamines (small-molecule neurotransmitters derived from tyrosine) are ~100-fold higher (*28–30*). Excitation with much deeper UV light (200- to 220-nm region) would access the larger cross section $S_0 \rightarrow S_2$ transitions and would provide greater isolation between the excitation and emission wavelengths. Unfortunately, efficient $S_2$ excitation has been impeded until recently by a dearth of reliable, low-noise lasers operating in this spectral region. In addition, high-NA microscope objectives—optics commonly used to improve mass detection limits by minimizing confocal probe volumes—typically are not engineered to transmit wavelengths shorter than ~350 nm.

We evaluated MPE fluorescence as a means to probe mixtures of catecholamines fractionated by CE and found this approach powerful for detecting small quantities of material (*31*). Because the 3PE-fluorescence cross sections for catecholamines are extremely small, the fundamental output of a Ti:S laser was frequency-doubled to produce ultrashort pulses of violet light in the expectation that two-photon excitation would be useful in high-sensitivity assays. Consistent with results from other laboratories that showed substantial two-photon excitation cross sections for tyrosinamide in the mid-400-nm region (*14*), we found that dopamine and epinephrine could be efficiently excited using 410-nm light. Moreover, catecholamine fluorescence ($\lambda_{max} \approx 305$ nm) could be measured with extremely low background by using highly efficient, colored-glass filters (UG11) with discrimination ratios $>10^5$. Such absorption-type filters often yield prohibitive autofluorescence in single-photon excitation experiments but could be used with impunity in these studies because the high-intensity dependence of multiphoton absorption confines efficient excitation to the sample region. In addition, the relatively intense "deep-UV" transitions could be excited with visible light, making it possible to use high-NA optics to focus the laser beam at the outlet of a 2-μm i.d. separation capillary. Mass detection limits achieved for this approach were ~100-fold lower than those previously obtained for UV-excited fluorescence of catecholamines, and they could be improved to ~1 amol for both dopamine and epinephrine by using a low dielectric constant solvent to reduce the photoionization quantum yield.

*MPE fluorescence complements other bioanalytical techniques but will not entirely supplant existing approaches.*

## Photochemistry

Confinement of multiphoton excitation to coordinates in proximity to a tightly focused laser beam provides a means to perform photochemistry in volumes as small as ~1 fL. This can be particularly useful in chemically generating biologically active molecules or ions from "caged" (chemically bound) precursors at highly localized positions within or outside cultured cells. Although this technique is still in relatively early stages of development, 2PE "point" photochemistry has been used for uncaging calcium ions (*32*) and neurotransmitters (*33*). In elegant studies, Denk and co-workers at Bell Laboratories was able to uncage acetylcholine (ACh) at well-defined sites outside cultured BC3H1 cells, and to map the surface density of ACh-gated ion channels by using patch-clamp techniques. To a certain extent, the future utility of this approach depends on the development of new caged species with appropriate chemical and multiphoton photophysical properties (*34*).

For many fluorophores, photobleaching reaction pathways can be more significant when using multiphoton excitation, thus limiting the total fluorescence signal per molecule. Although generally a drawback, in some instances facile MPE photochemistry can be used to enhance the detectability of biological analytes.

We investigated a novel, multiphoton-induced photochemical transformation that yields highly fluorescent visible-emitting compounds from hydroxyindoles and other indole derivatives (*35, 36*). This process requires absorption of three to four photons of Ti:S light (total energy requirement ≈ 6 eV) and yields products that can be excited with two additional Ti:S photons to produce a broad emission centered at ~500 nm. Because the photoreactivity of these products appears to be substantially lower than for the parent hydroxyindoles, this photochemical approach is an attractive alternative for high-

sensitivity analysis. Approximately 40,000 molecules of 5HT could be detected at the outlet of 620-nm i.d. electrophoresis channels using MPE photochemistry, a 20-fold improvement over UV-excited fluorescence and several fold better than could be achieved by using 2PE- or 3PE-UV fluorescence. Studies are in progress to clarify the photochemistry of this process with the goal of improving the photoconversion efficiency. In recent studies, we have observed that a similar process can be used to generate visible photoproducts from trihydroxyindole derivatives of epinephrine and norepinephrine.

## Conclusion

Multiphoton excitation through virtual-state intermediates was first demonstrated in the early 1960s (*37*) and was used occasionally in analytical laboratories in the 1970s and 1980s (*8, 10, 38*). In the past decade, MPE fluorescence has taken dramatic steps toward becoming a standard tool in bioanalytical analyses. Numerous applied physicists and physical chemists have helped to define the new capabilities afforded by multiphoton excitation in areas such as fluorescence anisotropy measurements, excitation of vacuum-UV chromophores in solution, and determination of macromolecular aggregation in dilute solutions (*5, 39, 40*).

Currently, the cost of Ti:S lasers presents a substantial barrier to further dissemination of this technology. Nevertheless, a "no-frills" Ti:S system (including pump laser) can be acquired for less than the cost of a large-frame argon laser and provides equal or greater versatility as a source for many UV and visible chromophores (often without the need to change the output wavelength). Moreover, the prospects appear good for further reductions in cost for limited-tunability and low-power Ti:S systems.

MPE fluorescence is a powerful complement to other bioanalytical techniques but certainly will not entirely supplant existing approaches. There are many circumstances in which single-photon confocal scanning microscopy yields equivalent or better results than does multiphoton microscopy, and it can do so for substantially less money. It is unlikely that femtosecond laser sources will be as affordable as low-power continuous-output lasers any time soon. In addition, the excellent mass detection limits achieved with MPE fluorescence—important for volume-limited applications such as single-cell analysis—can be less important in many situations than extremely low concentration detection limits. In general, low concentration detection limits can be achieved more readily by examining volumes of solution substantially larger than those efficiently probed with MPE fluorescence. However, with judiciously chosen applications, MPE fluorescence can offer advantages in the characterization of biological samples.

I am indebted to my present and former co-workers at the University of Texas and Cornell University for experimental and intellectual contributions and to W. Denk for contributing Figure 3. Financial support from the Arnold & Mabel Beckman Foundation, the Searle Scholars Program, the Welch Foundation, the Texas ATP, the NSF, and the ONR is gratefully acknowledged.

## References

(1) Callis, P. R. *Annu. Rev. Phys. Chem.* **1997,** *48,* 271–97.
(2) Xu, C.; Webb, W. W. In *Topics in Fluorescence Spectroscopy: Nonlinear and Two-Photon Induced Fluorescence*; Lakowicz, J. R., Ed.; Plenum Press: New York, 1997; Vol. 5; pp 471–537.
(3) McClain, W. M. *Acc. Chem. Res.* **1974,** *7,* 129–35.
(4) Lakowicz, J. R.; Gryczynski, I. In *Topics in Fluorescence Spectroscopy: Nonlinear and Two-Photon Induced Fluorescence*; Lakowicz, J. R., Ed.; Plenum Press: New York, 1997; Vol. 5; pp 87–139.
(5) Callis, P. R. In *Topics in Fluorescence Spectroscopy: Nonlinear and Two-Photon Induced Fluorescence*; Lakowicz, J. R., Ed.; Plenum Press: New York, 1997; Vol. 5; pp 1–39.
(6) Masthay, M. B.; Findsen, L. A.; Pierce, B. M.; Bocian, D. F.; Lindsey, J. S.; Birge, R. R. *J. Chem. Phys.* **1986,** *84,* 3901–15.
(7) Wright, J. C.; LaBuda, M. J.; Thompson, D. E.; Lascola, R.; Russell, M. W. *Anal. Chem.* **1996,** *68,* 600 A–607 A.
(8) Wirth, M. J.; Lytle, F. E. Two-Photon Excited Molecular Fluorescence. In *New Applications of Lasers to Chemistry;* Hieftje, G. M., Ed.; ACS Symposium Series 85; American Chemical Society: Washington, DC, 1978; pp 24–49.
(9) Wirth, M. J.; Fatunmbi, H. O. *Anal. Chem.* **1990,** *62,* 973–76.
(10) Sepaniak, M. J.; Yeung, E. S. *Anal. Chem.* **1977,** *49,* 1554–56.
(11) Hell, S. W.; Booth, M.; Wilms, S.; Schnetter, C. M.; Kirsch, A. K.; Arndt-Jovin, D. J.; Jovin, T. M. *Opt. Lett.* **1998,** *23,* 1238–40.
(12) Spence, D. E.; Kean, P. N.; Sibbett, W. *Opt. Lett.* **1991,** *16,* 42.
(13) Xu, C.; Webb, W. W. *J. Opt. Soc. Am. B* **1996,** *13,* 481–91.
(14) Rehms, A. A.; Callis, P. R. *Chem. Phys. Lett.* **1993,** *208,* 276–82.
(15) Maiti, S.; Shear, J. B.; Zipfel, W.; Williams, R. M.; Webb, W. W. *Science* **1997,** *275,* 530–32.
(16) Kierdaszuk, B.; Gryczynski, I.; Modrak-Wojcik, A.; Bzowska, A.; Shugar, D.; Lakowicz, J. R. *Photochem. Photobiol.* **1995,** *61,* 319–24.
(17) Xu, C.; Zipfel, W.; Shear, J. B.; Williams, R. M.; Webb, W. W. *Proc. Natl. Acad. Sci. U.S.A.* **1996,** *93,* 10,763–68.
(18) Albota, M., et al. *Science* **1998,** *281,* 1653–56.
(19) Schonle, A.; Hell, S. W. *Opt. Lett.* **1998,** *23,* 325–27.
(20) Denk, W.; Strickler, J. H.; Webb, W. W. *Science* **1990,** *248,* 73–76.
(21) *The Handbook of Confocal Microscopy*; Pawley, J., Ed.; Plenum Press: New York, 1995.
(22) Kleinfeld, D.; Mitra, P. P.; Helmchen, F.; Denk, W. *Proc. Natl. Acad. Sci. U.S.A.* **1998,** *95,* 15741–46.
(23) Gostkowski, M. L.; McDoniel, J. B.; Wei, J.; Curey, T. E.; Shear, J. B. *J. Am. Chem. Soc.* **1998,** *120,* 18–22.
(24) Williams, R. M.; Shear, J. B.; Zipfel, W.; Maiti, S.; Webb, W. W. *Biophys. J.* **1999,** *76,* 1835–46.
(25) Oliver, J. M.; Seagrave, J.; Stump, R. F.; Pfeiffer, J. R.; Deanin, G. G. *Prog. Allergy* **1988,** *42,* 185–245.
(26) Kim, T. D.; Eddlestone, G. T.; Mahmoud, S. F.; Kuchtey, J.; Fewtrell, C. *J. Biol. Chem.* **1997,** *272,* 31225–29.
(27) Tan, W.; Parpura, V.; Haydon, P. G.; Yeung, E. S. *Anal. Chem.* **1995,** *67,* 2575–79.
(28) Lillard, S. J.; Yeung, E. S.; McCloskey, M. A. *Proc. SPIE-Int. Soc. Opt. Eng.* **1997,** *2980,* 133–44.
(29) Timperman, A. T.; Oldenburg, K. E.; Sweedler, J. V. *Anal. Chem.* **1995,** *67,* 3421–26.
(30) Chang, H. T.; Yeung, E. S. *Anal. Chem.* **1995,** *67,* 1079–83.
(31) Gostkowski, M. L.; Shear, J. B. *J. Am. Chem. Soc.* **1998,** *120,* 12966–67.
(32) Brown, E. B.; Shear, J. B.; Adams, S. R.; Tsien, R. Y.; Webb, W. W. *Biophys. J.* **1999,** *76,* 489–99.
(33) Denk, W. *Proc. Natl. Acad. Sci. U.S.A.* **1994,** *91,* 6629–33.
(34) Toshiaki, F.; Wang, S. S.-H.; Dantzker, J. L.; Dore, T. M.; Bybee, W. J.; Callaway, E. M.; Denk, W.; Tsien, R. Y. *Proc. Natl. Acad. Sci. U.S.A.* **1999,** *96,* 1193–1200.
(35) Shear, J. B.; Xu, C.; Webb, W. W. *Photochem. Photobiol.* **1997,** *65,* 931–36.
(36) Gostkowski, M. L.; Wei, J.; Shear, J. B. *Anal. Biochem.* **1998,** *260,* 244–50.
(37) Kaiser, W.; Garrett, C. G. B. *Phys. Rev. Lett.* **1961,** *7,* 229.
(38) Pfeffer, W. D.; Yeung, E. S. *Anal. Chem.* **1986,** *58,* 2103–05.
(39) Dellonte, S.; Gardini, E.; Barigelletti, F.; Orlandi, G. *Chem. Phys. Lett.* **1977,** *49,* 596–98.
(40) Berland, K. M.; So, P. T. C.; Chen, Y.; Mantulin, W. W.; Gratton, E. *Biophys. J.* **1996,** *71,* 410–42.

*Jason B. Shear is an assistant professor in Chemistry and a fellow at the Institute for Cellular and Molecular Biology at the University of Texas. Address correspondence regarding this article to Shear at the University of Texas, Department of Chemistry and Biochemistry, Austin, TX 78712 (jshear@icmb.utexas.edu).*